

---

This is an electronic reprint of the original article.  
This reprint may differ from the original in pagination and typographic detail.

Author(s): Susi, Toma & Nasibulin, Albert G. & Jiang, Hua & Kauppinen, Esko I.  
Title: CVD Synthesis of Hierarchical 3D MWCNT/Carbon-Fiber Nanostructures  
Year: 2008  
Version: Final published version

**Please cite the original version:**

Susi, Toma & Nasibulin, Albert G. & Jiang, Hua & Kauppinen, Esko I. 2008. CVD Synthesis of Hierarchical 3D MWCNT/Carbon-Fiber Nanostructures. Journal of Nanomaterials. Volume 2008. 425195/1-7. ISSN 1687-4110 (printed). DOI: 10.1155/2008/425195

Rights: © 2008 Authors. This is an open access article distributed under the Creative Commons Attribution License, which permits unrestricted use, distribution, and reproduction in any medium, provided the original work is properly cited.

---

All material supplied via Aaltodoc is protected by copyright and other intellectual property rights, and duplication or sale of all or part of any of the repository collections is not permitted, except that material may be duplicated by you for your research use or educational purposes in electronic or print form. You must obtain permission for any other use. Electronic or print copies may not be offered, whether for sale or otherwise to anyone who is not an authorised user.

## Research Article

# CVD Synthesis of Hierarchical 3D MWCNT/Carbon-Fiber Nanostructures

Toma Susi,<sup>1,2</sup> Albert G. Nasibulin,<sup>1,2</sup> Hua Jiang,<sup>1,2</sup> and Esko I. Kauppinen<sup>1,2,3</sup>

<sup>1</sup>NanoMaterials Group, Department of Applied Physics, Helsinki University of Technology, P.O. Box 5100, Puumiehenkuja 2, 02015 TKK, Finland

<sup>2</sup>Center for New Materials, Helsinki University of Technology, P.O. Box 3500, Tietotie 3, 02015 TKK, Finland

<sup>3</sup>VTT Biotechnology, P.O. Box 1500, Tietotie 2, 02044 Espoo, Finland

Correspondence should be addressed to Albert G. Nasibulin, albert.nasibulin@tkk.fi

Received 12 May 2008; Accepted 11 September 2008

Recommended by Michael Wong

Multiwalled carbon nanotubes (MWCNTs) were synthesized by CVD on industrially manufactured highly crystalline vapor-grown carbon fibers (VGCFs). Two catalyst metals (Ni and Fe) and carbon precursor gases ( $C_2H_2$  and CO) were studied. The catalysts were deposited on the fibers by sputtering and experiments carried out in two different reactors. Samples were characterized by electron microscopy (SEM and TEM). Iron was completely inactive as catalyst with both  $C_2H_2$  and CO for reasons discussed in the paper. The combination of Ni and  $C_2H_2$  was very active for secondary CNT synthesis, without any pretreatment of the fibers. The optimal temperature for CNT synthesis was  $750^\circ C$ , with total gas flow of  $650\text{ cm}^3\text{min}^{-1}$  of  $C_2H_2$ ,  $H_2$ , and Ar in 1.0:6.7:30 ratio.

Copyright © 2008 Toma Susi et al. This is an open access article distributed under the Creative Commons Attribution License, which permits unrestricted use, distribution, and reproduction in any medium, provided the original work is properly cited.

## 1. INTRODUCTION

Carbon nanotubes (CNTs) have in recent years stimulated intensive scientific research due to their exceptional physical and chemical properties [1, 2]. A few different techniques, such as carbon arc-discharge [3, 4], laser ablation [5, 6], and substrate supported and aerosol chemical vapor deposition (CVD) [7–13], have been successful in producing lab-scale quantities of material.

CNT components have been used in a large range of applications: in light-emitting diodes [14], transistors [15], filters [16], field emitters [17], and photovoltaic devices [18]. Most of the proposed applications utilize the unique high strength, small size, large aspect ratio and surface area, and the exceptional chirality-determined electrical properties of nanotubes. In particular, the advantages gained by incorporating CNTs in fuel cells [19–22] and supercapacitors [23, 24] rely on the tubes' characteristic high surface area, combined with their good electrical conductivity.

Vapor-grown carbon fibers (VGCFs) are a type of carbon fiber produced by the CVD method, similar to nanotube synthesis [25]. A specific manufacturing process [26] commercialized by Showa Denko yields industrial-scale amounts

of high quality material. Many promising applications for VGCFs have been implemented in, for example, fuel cells [27], supercapacitors [28], and polymer composites [29].

Materials combining structures of different-size scales can be called hierarchical. The special case considered in this study is a combination of structures on two different-size scales: long, large diameter primary (or “first generation”) nanofibers, and shorter, smaller diameter secondary (or “second generation”) carbon nanotubes, attached to the primary fibers. Using the nomenclature of Teo and Sun [30], this can be characterized as the hierarchical “1D on 1D” structure  $CNT \rightarrow VGCF$ . The secondary tubes could, theoretically, be either multiwalled or single-walled.

In addition to work published about CNT growth on graphite [31], carbon cloth or paper [32–34], and MWCNTs [35, 36], carbon nanotubes have previously been synthesized on various carbon fibers [33, 37–42].

Most of the above methods either require complicated procedures for preparing suitable catalyst particles or extensive pretreatment of the fibers, or produce low yields and poor-quality tubes. We provide a simple method for synthesizing CNTs on untreated industrially manufactured highly crystalline Showa Denko VGCFs, and further study

the role of catalyst particles and precursor gases. Two catalyst metals—nickel and iron—were studied, with two carbon precursor gases, namely carbon monoxide (CO) and acetylene ( $C_2H_2$ ), used in two different reactors. Iron was found to be totally inactive for secondary tube growth, while nickel proved very active at suitable conditions.

## 2. RESULTS AND DISCUSSION

### 2.1. Acetylene experiments

The effect of various experimental parameters was extensively studied in the horizontal reactor used (Section 3.2), and a successful combination was found. Practically, no secondary nanotubes were produced at  $650^\circ C$ , confirming the findings of Duesberg et al. [43]. Of the three higher temperatures studied ( $700$ ,  $750$  and  $800^\circ C$ ), the best results were clearly obtained at  $750^\circ C$ . As for reduction time, the shortest tested period of 2.5 minutes seemed to be too short to form good catalyst particles, as activation (defined as a visual estimation of the density and length of produced secondary tubes in SEM) was poor. A reduction time of 5 minutes—which has been successfully utilized for iron [44] in a different setup—worked best with nickel. Based on 24 catalyst particles measured from TEM images of the 5-minute samples, the average diameter of nickel particles after synthesis on the Showa Denko fibers was  $9.5 \pm 1.9$  nm, while on the grid surface their average diameter was only  $5.5 \pm 1.3$  nm. After 7.5 minutes of reduction even though activation was in some places good, the produced secondary tubes were very short. Moreover, many particle sites were inactive and covered with amorphous carbon. The effect of gas composition was found to be less important within the range we studied, and the optimum flow rates were determined to be 30, 200, and  $420 \text{ cm}^3 \text{ min}^{-1}$  for acetylene, hydrogen, and argon, respectively.

In order to investigate the timeline of CNT growth, we carried out experiments for different synthesis times. The samples were prepared in the same manner as before (Section 3.1), but acetylene and hydrogen flows were stopped at the allotted time instead of the typical 10 minutes, and the reactor temperature was lowered. SEM observations showed that after 2.5 minutes of synthesis, growth has just barely begun, with very little activation on the Showa Denko fibers. After 5 minutes, activation was already significant, but the lengths of the synthesized secondary tubes were short. Activation after 15 minutes was significantly higher than activation after 10 minutes, suggesting that the growth was still proceeding at some rate after 10 minutes. The difference between 15- and 20-minute samples was not clear by visual observation. This behavior is in agreement with the findings of Krestinin et al. for methane pyrolysis [38].

In the optimal synthesis conditions, the VGCFs were well covered with secondary multiwalled tubes (Figure 1). Some secondary tubes had catalyst particles embedded at their ends, as found by TEM observation (Figure 2(a)). Most of them had between 10–20 walls and reasonably good wall structure (Figure 2(b)). A statistical survey of 20 MWCNTs

observed in TEM found the average outer diameter to be  $12.5 \pm 1.7$  nm, while the inner was  $5.2 \pm 2.0$  nm.

Switching to iron catalyst and using the same gas mixture that had proven successful with nickel, synthesis was attempted at temperatures of  $700$ ,  $750$ , and  $800^\circ C$ . The catalyst particles on the  $SiO_2$  substrate activated CNT growth effectively, with activation increasing with temperature. However, activation of the catalyst particles on the VGCFs was nonexistent. The good activation on the substrate itself proves that reactor conditions were perfectly suitable for growing tubes with acetylene from the iron catalysts. Furthermore, at the synthesis temperature of  $800^\circ C$ , carbon nanotube forests were grown from iron catalyst on the  $SiO_2$  substrate. At many places on the substrate, forests of several hundred micrometers in height were growing directly adjacent to the catalyst-containing fibers on which the catalysts were totally inactive (Figure 3).

### 2.2. Carbon monoxide experiments

Experiments with carbon monoxide using the vertical reactor (Section 3.3) with iron catalyst were unsuccessful in producing hierarchical structures. The iron catalyst particles were again completely inactive on the fibers. We carried out statistical measurements from TEM images of the samples prepared with 5-minute reduction and 30-minute growth time at  $890^\circ C$ . We measured 72 inactive iron particles: 40 on the Showa Denko fibers and 32 on the grid surface. The average diameter of iron particles on the fibers was  $13.5 \pm 2.7$  nm, while on the grid surface it was  $6.4 \pm 1.4$  nm.

### 2.3. Discussion

Synthesis of hierarchical nanostructures using iron catalyst was consistently unsuccessful with both carbon monoxide and acetylene. Variation of the experimental conditions together with the prolongation of synthesis time up to 2 hours did not result in any significant improvement. However, as noted above, reactor conditions were obviously appropriate for the CNT growth at least in the case of acetylene and iron, since CNT forests were successfully synthesized on the silicon wafer in the close vicinity of inactive fibers (Figure 3).

Let us discuss possible reasons for the catalytic inactivity of iron for the formation of secondary tubes on the surface of untreated Showa Denko VGCFs, and compare them with successful experiments with nickel and literature data. It is worth noting that in spite of the similarities between Fe and Ni, some of their properties are significantly different. Of main interest here, the solubility of carbon in bulk iron is much higher than that in nickel [45, 46]. Size effects alter the properties of Fe [47, 48] and Ni [49] nanoparticles significantly from those in the bulk. However, even for small nanoparticles, crucial differences between the two metals are preserved, with Amara et al. [49] explicitly underlining the importance of limited carbon solubility in Ni. Also, with iron, the higher solubility can result in the rapid formation of iron carbide, which is—conversely to nickel carbide—quite stable at the experimental conditions [50]. The formation

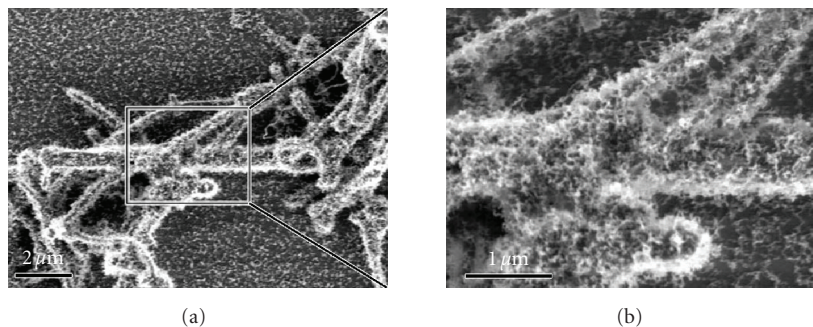


FIGURE 1: SEM images showing the morphology of produced MWCNTs on the Showa Denko carbon fibers. The sample was grown for 10 minutes using Ni and  $C_2H_2$  at  $750^\circ C$  with optimal gas composition, supported on an  $SiO_2$  substrate. (b) is a close-up of the area indicated in (a) Imaged using Leo Gemini DSM982 SEM.

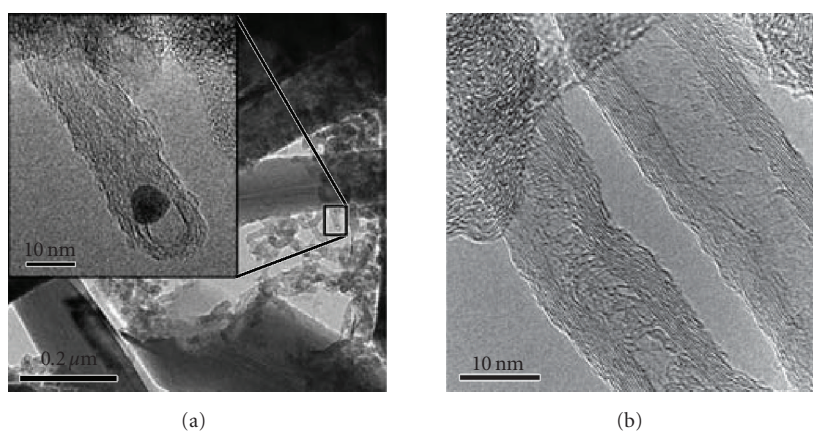


FIGURE 2: TEM images of Showa Denko fibers and the produced secondary tubes, grown with Ni and  $C_2H_2$  for 20 minutes at  $750^\circ C$  with optimal gas composition: (a) VGCFs and secondary MWCNTs. The inset is a close-up of the end of a secondary MWCNT, showing an encapsulated Ni catalyst particle. (b) Two different secondary MWCNTs. Imaged using Philips CM200 FEG TEM.

of iron carbide has been proposed to poison the catalyst [51, 52], inhibiting CNT growth [9, 53]. This view has been called into question, however, by recent in situ TEM observations of nanotube growth from  $Fe_3C$  nanoparticles [54].

Another reason for different products can be attributed to the different diffusion of catalyst particles on the VGCFs surfaces. Iron particles coalesced during the reduction step and CNT growth initiation period, producing excessively large particles for CNT growth. As mentioned above, the average diameter of both Fe and Ni catalyst particles was much larger on the Showa Denko fiber surfaces than on the TEM grid surface after synthesis (13.5 and 9.5 nm on the fibers and 6.4 and 5.5 nm on the grids for Fe and Ni, resp.). However, it is further evident that the Fe particles on the fibers were significantly larger than the Ni particles. Theoretical considerations [55] would expect particles of the sizes observed to be solid, especially at  $750^\circ C$  used in the acetylene experiments.

However, as noted in [55], observing the size of catalyst particles either before or after synthesis will not give a realistic picture of their true state during synthesis, as it is known that they are not static during reduction and

nucleation. In situ measurements would be needed to observe the evolution of the catalyst particle sizes during reduction and synthesis, and possible implications to the state of the particles and their inactivity. It is noteworthy that shortening the reduction period in either the  $Fe/C_2H_2$  or the  $Fe/CO$  experiments did not enable the production secondary tubes.

Importantly, data found in the literature indicates that pretreatment of the supporting carbon structure is vital when using iron [38, 56], as illustrated by the works listed in Table 1. The table displays a collection of relevant parameters from experiments successful in the synthesis of secondary nanotubes from iron catalyst on carbon fibers [33, 37–42]. Several successful special CVD methods are also included.

As an example, Zhu et al. [41] have demonstrated that there exists a limited temperature range where CNTs can grow from iron particles on noncrystalline carbon fibers, using low pressure methane gas as carbon precursor. At low temperatures, only a carbon layer is formed on the fiber surface. At higher temperature, the diffusion rate of iron particles into carbon fibers is enhanced. Small particles diffuse into the fibers before the carbon precursor is introduced, while larger ones nucleate only carbon clusters.



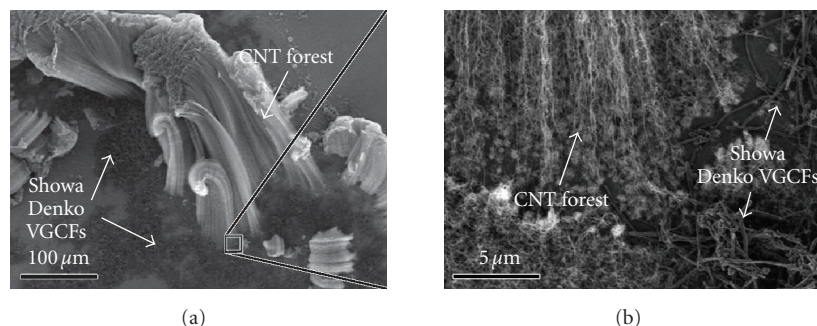


FIGURE 3: SEM images of CNT forests grown on  $\text{SiO}_2$  substrate from Fe catalyst with  $\text{C}_2\text{H}_2$  at  $800^\circ\text{C}$  with optimal gas composition: (a) Nanotube forest of about  $300\ \mu\text{m}$  in height growing from the substrate right next to the Showa Denko fibers. (b) Magnified image of the roots of the nanotube forest. The adjacent VGCFs were inactive for the growth of secondary tubes.

TABLE 1: Pretreatment conditions and special synthesis methods found in the literature, which have enabled iron-catalyzed secondary CNT growth on various carbon materials. CF = carbon fibers, CP = carbon paper.

Support (supplier)	Treatment/method	Catalyst precursor	Carbon source	T [ $^\circ\text{C}$ ]	Ref.
CP (E-tech)	PECVD	e-beam Fe	Methane	600	[33]
CF (Toray)	Injection	Ferrocene	Toluene	750	[37]
CF	Acid bath	$\text{Fe}(\text{NO}_3)_3$	Acetylene	750	[38]
CP (Toray)	Injection, $\text{H}_2\text{S}$	Ferrocene	Xylene	800	[39]
CF	Injection	Ferrocene	Xylene	800	[40]
CF	Reduced pressure	Ferrofluid	Methane	750	[41]
CP (E-TEK)	Ohmic heating	$\text{Fe}(\text{NO}_3)_3$	Ethylene	700	[42]

The case above and most of the others listed in Table 1 differ from our experiments either by a radically modified CVD procedure or by the lower crystallinity of the supporting fiber—a property which is altered by pretreatment. A more crystalline support could affect both proper carbon diffusion and the diffusion of catalyst particles on the fibers. Interestingly, Li et al. [31] have found that when growing CNTs from a stainless steel film was deposited on a graphite foil surface, phase segregation happens during the formation of catalyst particles, and only Fe/Ni alloy particles rich in Ni are responsible for the CNTs growth.

### 3. EXPERIMENTAL

#### 3.1. Sample preparation

For our supported CVD synthesis of hierarchical carbon nanostructures, industrially manufactured Showa Denko VGCFs were used as the primary level of the hierarchical structure. The tubes were delivered as a powder of very crystalline and pure nanofibers with an average diameter of around  $150\ \text{nm}$ . The fibers were dispersed in (1,2)-dichloroethane (DCE) in a low-power ultrasonic bath at  $40\text{--}50^\circ\text{C}$ , with concentrations ranging from  $0.5$  to  $1.5\ \text{mg/mL}^{-1}$ .

For acetylene experiments, silicon wafers were used to support the VGCFs. The sizes of the substrates cut from the wafers were about  $0.5\ \text{cm}^2$ . The pieces were cut from either

a (111)  $\text{SiO}_2/\text{Si}$  wafer with a thermally grown  $260\ \text{nm}$   $\text{SiO}_2$  layer, or from a (100) Si wafer with a native oxide layer. Droplets of DCE solution of VGCF material were deposited on the substrate surfaces by drop-drying. After synthesis, all samples were observed by field emission scanning electron microscope (Leo Gemini DSM982). Selected samples were also observed by field emission transmission electron microscope (Philips CM200 FEG) after transferring the fabricated material onto TEM grids (SPI, 100 Ni  $\text{SiO}_2/\text{SiO}$ ). This was done by wetting the silicon substrate surfaces with DCE and wiping them with TEM grids. For carbon monoxide experiments, the samples were grown directly on TEM grids, which were inserted into a vertical reactor using a specially designed holder.

Sputtering was used to deposit the catalyst particles needed for the CVD synthesis. For the  $\text{C}_2\text{H}_2$  experiments, the sputtering targets used were nickel and iron, while iron was used for synthesis with CO. A magnetron sputter coater (AGAR Auto Sputter Coater 108A) was used to produce nanoparticles on the carbon fibers deposited on the substrates. A sputtering current of  $20\ \text{mA}$  maintained for 15 seconds was used for both targets, as this has been found to be optimal for CNT production with the reactors used [57].

#### 3.2. Acetylene reactor

The synthesis of carbon nanotubes with  $\text{C}_2\text{H}_2$  was carried out in a horizontal reactor. It consisted of a  $40\ \text{cm}$  long quartz

tube with an inner diameter of 1.2 cm, set inside a ceramic tube with an inner diameter of 3.0 cm. The tube was further placed inside a 34 cm long furnace, which was heated to a high temperature needed for the synthesis. Temperature calibration was done with a digital thermometer (Fluke 52 K/J) attached to a K-type metal wire thermocouple. The temperature inside the reactor at growth conditions was measured to be constant for a distance of several centimeters around the sample position.

For the synthesis, the samples were put into a ceramic boat, one end of the tube opened, and the boat pushed to the high temperature zone of the reactor with a steel rod. The reactor was then sealed. Before the introduction of the carbon source gas, deposited Ni or Fe catalysts were reduced at the selected synthesis temperature in a hydrogen-containing atmosphere, typically for 5 minutes. After reduction, acetylene was introduced and kept at a constant flow for the desired period of time (typically 10 minutes). The flows were controlled using a mass flow controller (Aalborg GFC17) or critical orifices calibrated with a flow calibrator (Gilian Gilibrator-2).

After the synthesis period, acetylene and hydrogen flows were stopped and the reactor temperature was lowered. Argon flow rate was increased to  $700 \text{ cm}^3 \text{ min}^{-1}$  to hasten the cooling. After a cooling period of about 1.5 hours, at which point the sample temperatures were well below  $200^\circ\text{C}$ , the ends of the quartz tube were opened and the boat pushed out of the quartz tube with the steel rod.

The main parameters varied in the acetylene experiments were synthesis temperature ( $650\text{--}800^\circ\text{C}$ ), reduction time (2.5–7.5 minutes), acetylene flow rate ( $10\text{--}50 \text{ cm}^3 \text{ min}^{-1}$ , corresponding to concentrations of 1.6–13.0% depending on the gas mix), and synthesis time (2.5–20 minutes). Furthermore, in some experiments the flow rates of  $\text{H}_2$  (0, 130, and  $200 \text{ cm}^3 \text{ min}^{-1}$ ) and Ar (0, 270, 420, and  $700 \text{ cm}^3 \text{ min}^{-1}$ ) were varied to study the possible effects of mixing and gas composition.

### 3.3. Carbon monoxide reactor

The synthesis of CNTs with CO was attempted in a vertical laminar flow reactor. It consisted of a ceramic tube with an inner diameter of 2.2 cm inside a 44 cm long furnace. A stainless steel rod of 6 mm in diameter with a TEM grid holder at one end was used for inserting the samples. The reactor design and procedure for the CO experiments were identical to previous work [57].

Briefly, a temperature of  $890^\circ\text{C}$  had been found to be optimal for iron-catalyzed growth on  $\text{SiO}_2$  wafers, with a reduction time of 5 minutes with  $\text{H}_2$  and Ar flows ( $200$  and  $400 \text{ cm}^3 \text{ min}^{-1}$ ) passed into the reactor. Ar was then replaced with CO ( $400 \text{ cm}^3 \text{ min}^{-1}$ ), while the  $\text{H}_2$  flow remained constant. A small amount of  $\text{CO}_2$  ( $8 \text{ cm}^3 \text{ min}^{-1}$ ) was introduced into the reactor for the whole duration of the experiment, as this had been found to have a critical effect on nanotube growth [58]. In this study, typical synthesis times were 30 minutes, and the samples were characterized by SEM and TEM.

## 4. CONCLUSION

Two different carbon precursor gases, carbon monoxide and acetylene, were studied for the synthesis of secondary carbon nanotubes on the surface of highly crystalline Showa Denko vapor-grown carbon fibers. Two different catalyst metals were examined, namely nickel and iron with acetylene, and iron with carbon monoxide. Of these, the combination of nickel and acetylene proved to be the only working solution.

Using the presented simple and straightforward nickel-catalyzed synthesis on untreated VGCF surfaces, the achieved optimal secondary tube yield was high, with good activation and coverage on the carbon fibers. With view of applications, either replacing the Showa Denko fibers with multiwalled carbon nanotubes grown directly to a conducting substrate to act as the primary structure, or replacing the VGCFs used in current applications by our material would be logical next steps. Potential applications for this nanomaterial would include catalyst supports in fuel cells, powerful supercapacitors, and possibly gas sensors. One further interesting application could be the use of hierarchical nanostructures as reinforcement material. The secondary tubes could act as “anchors” to prevent the slipping of MWCNT or fiber composites, thus improving the mechanical properties significantly.

## ACKNOWLEDGMENTS

The authors thank Mr. Prasantha R. Mudimela for his help during sputtering condition investigations. The authors acknowledge the Academy of Finland for financial support (Grant no. 118445).

## REFERENCES

- [1] S. Reich, C. Thomsen, and J. Maultzsch, *Carbon Nanotubes: Basic Concepts and Physical Properties*, Wiley-VCH, Weinheim, Germany, 2004.
- [2] S. V. Rotkin and S. Subramoney, *Applied Physics of Carbon Nanotubes: Fundamentals of Theory, Optics and Transport Devices*, Springer, Berlin, Germany, 2008.
- [3] T. W. Ebbesen and P. M. Ajayan, “Large-scale synthesis of carbon nanotubes,” *Nature*, vol. 358, no. 6383, pp. 220–222, 1992.
- [4] S. Iijima and T. Ichihashi, “Single-shell carbon nanotubes of 1-nm diameter,” *Nature*, vol. 363, no. 6430, pp. 603–605, 1993.
- [5] T. Guo, P. Nikolaev, A. Thess, D. T. Colbert, and R. E. Smalley, “Catalytic growth of single-walled nanotubes by laser vaporization,” *Chemical Physics Letters*, vol. 243, no. 1–2, pp. 49–54, 1995.
- [6] I. G. Assovskii and G. I. Kozlov, “Synthesis of single-walled carbon nanotubes by the laser ablation of graphite under normal conditions,” *Doklady Physical Chemistry*, vol. 388, no. 1–3, pp. 13–17, 2003.
- [7] L. V. Radushkevich and V. M. Luk’yanovich, “The structure of carbon forming in thermal decomposition of carbon monoxide on an iron catalyst,” *Soviet Journal of Chemical Physics*, vol. 26, pp. 88–95, 1952.
- [8] P. Nikolaev, M. J. Bronikowski, R. K. Bradley, et al., “Gas-phase catalytic growth of single-walled carbon nanotubes

- from carbon monoxide,” *Chemical Physics Letters*, vol. 313, no. 1-2, pp. 91–97, 1999.
- [9] A. R. Harutyunyan, B. K. Pradhan, U. J. Kim, G. Chen, and P. C. Eklund, “CVD synthesis of single wall carbon nanotubes under “soft” conditions,” *Nano Letters*, vol. 2, no. 5, pp. 525–530, 2002.
- [10] K. Hata, D. N. Futaba, K. Mizuno, T. Namai, M. Yumura, and S. Iijima, “Water-assisted highly efficient synthesis of impurity-free single-walled carbon nanotubes,” *Science*, vol. 306, no. 5700, pp. 1362–1364, 2004.
- [11] A. G. Nasibulin, A. Moisala, D. P. Brown, H. Jiang, and E. I. Kauppinen, “A novel aerosol method for single walled carbon nanotube synthesis,” *Chemical Physics Letters*, vol. 402, no. 1–3, pp. 227–232, 2005.
- [12] G. Lolli, L. Zhang, L. Balzano, N. Sakulchaicharoen, Y. Tan, and D. E. Resasco, “Tailoring ( $n, m$ ) structure of single-walled carbon nanotubes by modifying reaction conditions and the nature of the support of CoMo catalysts,” *Journal of Physical Chemistry B*, vol. 110, no. 5, pp. 2108–2115, 2006.
- [13] A. Moisala, A. G. Nasibulin, D. P. Brown, H. Jiang, L. Khriachtchev, and E. I. Kauppinen, “Single-walled carbon nanotube synthesis using ferrocene and iron pentacarbonyl in a laminar flow reactor,” *Chemical Engineering Science*, vol. 61, no. 13, pp. 4393–4402, 2006.
- [14] C. M. Aguirre, S. Auvray, S. Pigeon, R. Izquierdo, P. Desjardins, and R. Martel, “Carbon nanotube sheets as electrodes in organic light-emitting diodes,” *Applied Physics Letters*, vol. 88, no. 18, Article ID 183104, 3 pages, 2006.
- [15] S. Auvray, V. Derycke, M. Goffman, A. Filoramo, O. Jost, and J.-P. Bourgoin, “Chemical optimization of self-assembled carbon nanotube transistors,” *Nano Letters*, vol. 5, no. 3, pp. 451–455, 2005.
- [16] A. Srivastava, O. N. Srivastava, S. Talapatra, R. Vajtai, and P. M. Ajayan, “Carbon nanotube filters,” *Nature Materials*, vol. 3, no. 9, pp. 610–614, 2004.
- [17] A. G. Nasibulin, P. V. Pikhitsa, H. Jiang, et al., “A novel hybrid carbon material,” *Nature Nanotechnology*, vol. 2, no. 3, pp. 156–161, 2007.
- [18] H. Ago, K. Petritsch, M. S. P. Shaffer, A. H. Windle, and R. H. Friend, “Composites of carbon nanotubes and conjugated polymers for photovoltaic devices,” *Advanced Materials*, vol. 11, no. 15, pp. 1281–1285, 1999.
- [19] W. Li, C. Liang, J. Qiu, et al., “Carbon nanotubes as support for cathode catalyst of a direct methanol fuel cell,” *Carbon*, vol. 40, no. 5, pp. 791–794, 2002.
- [20] C. Wang, M. Waje, X. Wang, J. M. Tang, R. C. Haddon, and Y. Yan, “Proton exchange membrane fuel cells with carbon nanotube based electrodes,” *Nano Letters*, vol. 4, no. 2, pp. 345–348, 2004.
- [21] M. Gangeri, S. Perathoner, and G. Centi, “Synthesis and performances of carbon-supported noble metal nanoclusters as electrodes for polymer electrolyte membrane fuel cells,” *Inorganica Chimica Acta*, vol. 359, no. 15, pp. 4828–4832, 2006.
- [22] C.-H. Wang, H.-C. Shih, Y.-T. Tsai, H.-Y. Du, L.-C. Chen, and K.-H. Chen, “High methanol oxidation activity of electrocatalysts supported by directly grown nitrogen-containing carbon nanotubes on carbon cloth,” *Electrochimica Acta*, vol. 52, no. 4, pp. 1612–1617, 2006.
- [23] S. J. Kang, C. Kocabas, T. Ozel, et al., “High-performance electronics using dense, perfectly aligned arrays of single-walled carbon nanotubes,” *Nature Nanotechnology*, vol. 2, no. 4, pp. 230–236, 2007.
- [24] V. L. Pushparaj, M. M. Shaijumon, A. Kumar, et al., “Flexible energy storage devices based on nanocomposite paper,” *Proceedings of the National Academy of Sciences of the United States of America*, vol. 104, no. 34, pp. 13574–13577, 2007.
- [25] M. Endo, “Grow carbon fibers in the vapor phase,” *CHEMTECH*, vol. 18, no. 9, pp. 568–576, 1988.
- [26] M. Endo, Y. A. Kim, T. Hayashi, et al., “Vapor-grown carbon fibers (VGCFs): basic properties and their battery applications,” *Carbon*, vol. 39, no. 9, pp. 1287–1297, 2001.
- [27] I. Yamanaka, T. Hashimoto, R. Ichihashi, and K. Otsuka, “Direct synthesis of H<sub>2</sub>O<sub>2</sub> acid solutions on carbon cathode prepared from activated carbon and vapor-growing-carbon-fiber by a H<sub>2</sub>/O<sub>2</sub> fuel cell,” *Electrochimica Acta*, vol. 53, no. 14, pp. 4824–4832, 2008.
- [28] J.-H. Kim, Y.-S. Lee, A. K. Sharma, and C. G. Liu, “Polypyrrole/carbon composite electrode for high-power electrochemical capacitors,” *Electrochimica Acta*, vol. 52, no. 4, pp. 1727–1732, 2006.
- [29] G. G. Tibbetts, M. L. Lake, K. L. Strong, and B. P. Rice, “A review of the fabrication and properties of vapor-grown carbon nanofiber/polymer composites,” *Composites Science and Technology*, vol. 67, no. 7-8, pp. 1709–1718, 2007.
- [30] B. K. Teo and X. H. Sun, “Classification and representations of low-dimensional nanomaterials: terms and symbols,” *Journal of Cluster Science*, vol. 18, no. 2, pp. 346–357, 2007.
- [31] W. Z. Li, D. Z. Wang, S. X. Yang, J. G. Wen, and Z. F. Ren, “Controlled growth of carbon nanotubes on graphite foil by chemical vapor deposition,” *Chemical Physics Letters*, vol. 335, no. 3-4, pp. 141–149, 2001.
- [32] X. Sun, B. Stansfield, J. P. Dodelet, and S. Désilets, “Growth of carbon nanotubes on carbon paper by Ohmically heating silane-dispersed catalytic sites,” *Chemical Physics Letters*, vol. 363, no. 5-6, pp. 415–421, 2002.
- [33] C.-C. Chen, C. F. Chen, C.-H. Hsu, and I.-H. Li, “Growth and characteristics of carbon nanotubes on carbon cloth as electrodes,” *Diamond and Related Materials*, vol. 14, no. 3–7, pp. 770–773, 2005.
- [34] S. H. Jo, J. Y. Huang, S. Chen, G. Y. Xiong, D. Z. Wang, and Z. F. Ren, “Field emission of carbon nanotubes grown on carbon cloth,” *Journal of Vacuum Science and Technology B*, vol. 23, no. 6, pp. 2363–2368, 2005.
- [35] X. Sun, R. Li, B. Stansfield, J. P. Dodelet, and S. Désilets, “3D carbon nanotube network based on a hierarchical structure grown on carbon paper backing,” *Chemical Physics Letters*, vol. 394, no. 4–6, pp. 266–270, 2004.
- [36] N. Li, X. Chen, L. Stoica, et al., “The catalytic synthesis of three-dimensional hierarchical carbon nanotube composites with high electrical conductivity based on electrochemical iron deposition,” *Advanced Materials*, vol. 19, no. 19, pp. 2957–2960, 2007.
- [37] R. B. Mathur, S. Chatterjee, and B. P. Singh, “Growth of carbon nanotubes on carbon fibre substrates to produce hybrid/phenolic composites with improved mechanical properties,” *Composites Science and Technology*, vol. 68, no. 7-8, pp. 1608–1615, 2008.
- [38] L. Zeng, W. Wang, D. Lei, et al., “The effect of carbon microfiber substrate pretreatment on the growth of carbon nanomaterials,” *Carbon*, vol. 46, no. 2, pp. 359–364, 2008.
- [39] N. Sonoyama, M. Ohshita, A. Nijubu, et al., “Synthesis of carbon nanotubes on carbon fibers by means of two-step thermochemical vapor deposition,” *Carbon*, vol. 44, no. 9, pp. 1754–1761, 2006.
- [40] Z.-G. Zhao, L.-J. Ci, H.-M. Cheng, and J.-B. Bai, “The growth of multi-walled carbon nanotubes with different morphologies on carbon fibers,” *Carbon*, vol. 43, no. 3, pp. 663–665, 2005.

- [41] S. Zhu, C.-H. Su, S. L. Lehoczky, I. Muntele, and D. Ila, "Carbon nanotube growth on carbon fibers," *Diamond and Related Materials*, vol. 12, no. 10-11, pp. 1825–1828, 2003.
- [42] O. Smiljanic, T. Dellerio, A. Serventi, et al., "Growth of carbon nanotubes on Ohmically heated carbon paper," *Chemical Physics Letters*, vol. 342, no. 5-6, pp. 503–509, 2001.
- [43] G. S. Duesberg, A. P. Graham, F. Kreupl, et al., "Ways towards the scaleable integration of carbon nanotubes into silicon based technology," *Diamond and Related Materials*, vol. 13, no. 2, pp. 354–361, 2004.
- [44] P. R. Mudimela, Submitted, 2008.
- [45] W. W. Dunn, R. B. McLellan, and W. A. Oates, "Solubility of carbon in cobalt and nickel," *Transactions of Nonferrous Metals Society of China*, vol. 242, no. 10, pp. 2129–2132, 1968.
- [46] J. Chipman, "Thermodynamics and phase diagram of the Fe-C system," *Metallurgical and Materials Transactions B*, vol. 3, no. 1, pp. 55–64, 1972.
- [47] A. R. Harutyunyan, N. Awasthi, A. Jiang, et al., "Reduced carbon solubility in Fe nanoclusters and implications for the growth of single-walled carbon nanotubes," *Physical Review Letters*, vol. 100, no. 19, Article ID 195502, 2008.
- [48] F. Ding and K. Bolton, "The importance of supersaturated carbon concentration and its distribution in catalytic particles for single-walled carbon nanotube nucleation," *Nanotechnology*, vol. 17, no. 2, pp. 543–548, 2006.
- [49] H. Amara, C. Bichara, and F. Ducastelle, "Understanding the nucleation mechanisms of carbon nanotubes in catalytic chemical vapor deposition," *Physical Review Letters*, vol. 100, no. 5, Article ID 056105, 2008.
- [50] M. Audier, M. Coulon, and L. Bonnetain, "Disproportionation of CO on iron-cobalt alloys—I: thermodynamic study," *Carbon*, vol. 21, no. 2, pp. 93–97, 1983.
- [51] R. T. K. Baker, J. R. Alonzo, J. A. Dumesic, and D. J. C. Yates, "Effect of the surface state of iron on filamentous carbon formation," *Journal of Catalysis*, vol. 77, no. 1, pp. 74–84, 1982.
- [52] S. Herreyre, P. Gadelle, P. Moral, and J. M. M. Millet, "Study by Mössbauer spectroscopy and magnetization measurement of the evolution of iron catalysts used in the disproportionation of CO," *Journal of Physics and Chemistry of Solids*, vol. 58, no. 10, pp. 1539–1545, 1997.
- [53] J. Gavillet, A. Loiseau, C. Journet, F. Willaime, F. Ducastelle, and J.-C. Charlier, "Root-growth mechanism for single-wall carbon nanotubes," *Physical Review Letters*, vol. 87, no. 27, Article ID 275504, 4 pages, 2001.
- [54] H. Yoshida, S. Takeda, T. Uchiyama, H. Kohno, and Y. Homma, "Atomic-scale in-situ observation of carbon nanotube growth from solid state iron carbide nanoparticles," *Nano Letters*, vol. 8, no. 7, pp. 2082–2086, 2008.
- [55] A. Moysala, A. G. Nasibulin, and E. I. Kauppinen, "The role of metal nanoparticles in the catalytic production of single-walled carbon nanotubes—a review," *Journal of Physics Condensed Matter*, vol. 15, no. 42, pp. S3011–S3035, 2003.
- [56] Y. Xia, L. Zeng, W. Wang, et al., "Synthesis and characterization of carbon nanotubes on carbon microfibers by floating catalyst method," *Applied Surface Science*, vol. 253, no. 16, pp. 6807–6810, 2007.
- [57] P. Queipo, A. G. Nasibulin, D. Gonzalez, et al., "Novel catalyst particle production method for CVD growth of single- and double-walled carbon nanotubes," *Carbon*, vol. 44, no. 8, pp. 1604–1608, 2006.
- [58] A. G. Nasibulin, D. P. Brown, P. Queipo, D. Gonzalez, H. Jiang, and E. I. Kauppinen, "An essential role of CO<sub>2</sub> and H<sub>2</sub>O during single-walled CNT synthesis from carbon monoxide," *Chemical Physics Letters*, vol. 417, no. 1–3, pp. 179–184, 2006.





**Hindawi**

Submit your manuscripts at  
<http://www.hindawi.com>

